Thermodynamic observables of Mn_{12}-acetate calculated for the full spin Hamiltonian

Oliver Hanebaum and Jürgen Schnack*
Fakultät für Physik, Universität Bielefeld, Postfach 100131, D-33501 Bielefeld, Germany
(Received 23 June 2015; published 27 August 2015)

Thirty-five years after its synthesis, magnetic observables are calculated for the molecular nanomagnet Mn_{12}-acetate using a spin Hamiltonian that contains all spins. Starting from a very advanced density functional theory parametrization [V. V. Mazurenko *et al.*, Phys. Rev. B **89**, 214422 (2014)], we evaluate magnetization and specific heat for this anisotropic system of 12 manganese ions with a staggering Hilbert space dimension of 100 000 000 using the finite-temperature Lanczos method. We compare the results with those obtained from other parametrizations. Our investigations demonstrate that it is now possible to assess the quality of parametrizations of effective spin Hamiltonians for rather large magnetic molecules.

DOI: 10.1103/PhysRevB.92.064424 PACS number(s): 75.10.Jm, 75.50.Xx, 75.40.Mg

I. INTRODUCTION

Density functional theory (DFT) has greatly advanced over the past years and is nowadays able to predict the parameters of spin Hamiltonians with which the low-temperature physics of correlated magnetic materials can be described (compare, e.g., Refs. [1–15]). Along this line, the complex spin Hamiltonian of one of the most exciting magnetic molecules, Mn_{12}-acetate, was recently predicted [16]. These calculations consider almost all terms that are bilinear in spin operators, such as the Heisenberg exchange interaction, the anisotropic antisymmetric exchange interaction, and single-ion anisotropy tensors. The new calculations outperform earlier attempts [17,18] and provide rich electronic insight. But despite all the success, DFT is not capable of evaluating magnetic observables, which is the reason for the detour via spin Hamiltonians. Alternative approaches to obtain parametrizations of spin Hamiltonians are given by fits to magnetic observables [19] or by assuming values known from similar but smaller systems.

The magnetism of anisotropic molecular spin systems is fascinating due to interesting phenomena such as bistability and quantum tunneling of the magnetization [20]. Bistability in connection with a small tunneling rate leads to a magnetic hysteresis of molecular origin in these systems. That is why such molecules are termed single molecule magnets (SMMs); Mn_{12}-acetate is the most prominent SMM [21–27]. But although Mn_{12}-acetate contains only four $Mn^{(IV)}$ ions with $s = 3/2$ and eight $Mn^{(III)}$ ions with $s = 2$, it constitutes a massive challenge for theoretical calculations in terms of spin Hamiltonians, since the underlying Hilbert space of dimension 100 000 000 is orders of magnitude too big for an exact and complete matrix diagonalization [28]. But, owing to the fact that the zero-field split ground-state multiplet is energetically separated from higher-lying levels, a description using only the $S = 10$ ground-state manifold is sufficient to explain observables at low temperature—this approach was used in the past. Thermodynamic functions which involve higher-lying levels, for instance, observables at higher temperatures, of course cannot be evaluated in such an approximation.

Fortunately, in past years, progress has been made on DFT as well as in terms of powerful approximations for spin-Hamiltonian calculations. For not too big systems with Hilbert spaces with dimensions of up to 10^{10}, Krylov space methods such as the finite-temperature Lanczos method (FTLM) have proven to provide astonishingly accurate approximations of magnetic observables [29–41]. While FTLM has been mostly used for Heisenberg spin systems, very recently the method was advanced to anisotropic spin systems [42].

In this paper we therefore employ the most recent FTLM in order to study the thermodynamic functions of Mn_{12}-acetate, starting from parametrizations provided by DFT or other methods. We evaluate both the magnetization as well as the specific heat as functions of temperature and field and compare the various parametrizations of the spin Hamiltonian.

The paper is organized as follows. In Sec. II the employed Hamiltonian as well as the basics of the finite-temperature Lanczos method are introduced. Sections III–V discuss the effective magnetic moment, the magnetization, and the specific heat, respectively. The paper closes with a summary and outlook.

II. FTLM FOR ANISOTROPIC SPIN SYSTEMS

For Mn_{12}-acetate, which is a highly anisotropic spin system, the complete Hamiltonian of the spin system is given by the exchange term, the single-ion anisotropy, and the Zeeman term, i.e.,

$$\underset{\sim}{H} = \sum_{i<j} \underset{\sim}{\vec{s}}_i \cdot \mathbf{J}_{ij} \cdot \underset{\sim}{\vec{s}}_j + \sum_i \underset{\sim}{\vec{s}}_i \cdot \mathbf{D}_i \cdot \underset{\sim}{\vec{s}}_i + \mu_B B \sum_i g_i \underset{\sim}{s}_i^z . \quad (1)$$

$\mathbf{J}_{ij}$ is a 3×3 matrix for each interacting pair of spins at sites i and j which contains the isotropic Heisenberg exchange parameters, together with the anisotropic symmetric and antisymmetric terms. In the sign convention of (1), a positive Heisenberg exchange corresponds to an antiferromagnetic interaction and a negative one to a ferromagnetic interaction. $\mathbf{D}_i$ denotes the single-ion anisotropy tensor at site i, which in its eigensystem $\vec{e}_i^{\,1}, \vec{e}_i^{\,2}, \vec{e}_i^{\,3}$ can be decomposed as

$$\mathbf{D}_i = D_i \vec{e}_i^{\,3} \otimes \vec{e}_i^{\,3} + E_i \left\{ \vec{e}_i^{\,1} \otimes \vec{e}_i^{\,1} - \vec{e}_i^{\,2} \otimes \vec{e}_i^{\,2} \right\}. \quad (2)$$

The terms g_i could in general be 3×3 matrices, too, but for the sake of simplicity it is assumed that the g_i are numbers

*jschnack@uni-bielefeld.de

and, moreover, that $g_i = 2$ for all ions. This assumption is justified for the $Mn^{(IV)}$ and $Mn^{(III)}$ ions in Mn_{12}-acetate, since the g factors of both ions are estimated to be very close to 2 [19,43–46]. Hamiltonian (1) has proven to be appropriate on very general grounds for many $3d$ magnetic ions with a not too strong spin-orbit interaction (strong exchange limit). For these cases, and in particular for $Mn^{(IV)}$ and $Mn^{(III)}$, it contains the dominant terms [20,47,48]. Sometimes higher-order spin operators such as, for instance, biquadratic terms are needed, for instance, in the case of some nickel compounds [47,49–56].

The finite-temperature Lanczos method (FTLM) approximates the partition function in two ways [29,30],

$$Z(T,B) \approx \frac{\dim(\mathcal{H})}{R} \sum_{\nu=1}^{R} \sum_{n=1}^{N_L} e^{-\beta\epsilon_n^{(\nu)}} |\langle n(\nu)|\nu\rangle|^2. \qquad (3)$$

The sum over a complete set of vectors is replaced by a much smaller sum over R random vectors $|\nu\rangle$. The exponential of the Hamiltonian is then approximated by its spectral representation in a Krylov space spanned by the N_L Lanczos vectors starting from the respective random vector $|\nu\rangle$. $|n(\nu)\rangle$ is the nth eigenvector of $\underset{\sim}{H}$ in this Krylov space. It turns out that very good accuracy can already be achieved for parameters $R \approx 10$ and $N_L \approx 100$, especially in cases when the low-lying energy spectrum is dense [40,42].

III. EFFECTIVE MAGNETIC MOMENT AS A FUNCTION OF TEMPERATURE

Mn_{12}-acetate contains four $Mn^{(IV)}$ ions with $s = 3/2$ and eight $Mn^{(III)}$ ions with $s = 2$. Following Ref. [16], the ions and the exchange pathways are depicted in Fig. 1. $Mn^{(IV)}$ ions (1–4) are shown as red circles, and $Mn^{(III)}$ ions (5–12) as blue ones. An S_4 symmetry of the molecule is assumed [57].

Since the discovery of the pronounced SMM properties of Mn_{12}-acetate, several groups developed parametrizations of the full spin Hamiltonian. These data sets, of which the most prominent ones are given in Table I, contain parametrizations of Heisenberg models and were put forward following various scientific reasonings. Earlier attempts assigned values of exchange interactions in analogy to smaller compounds with similar chemical bridges between the manganese ions. Later investigations combined, for instance, high-temperature series expansion with the evaluation of low-lying excitations seen in inelastic neutron scattering (INS) experiments [19]. A necessary condition that has to be met by all parametrizations is that the ground state has a total spin of $S = 10$. The DFT parametrization of Ref. [16] is also compatible with INS experiments. Using an ordinary Lanczos procedure, the low-lying levels have been evaluated and presented in Ref. [16].

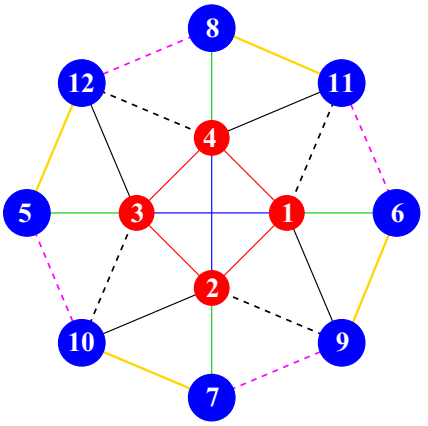

FIG. 1. (Color online) Schematic structure of Mn12; same labeling as in Ref. [16]. $Mn^{(IV)}$ ions (1–4) are shown as red circles, and $Mn^{(III)}$ ions (5–12) as blue ones. An S_4 symmetry is assumed.

TABLE I. Intramolecular isotropic exchange interaction parameters (in meV) as suggested by various authors (compare Ref. [16]). The spin labels are explained in Fig. 1.

No.	Bond $(i\text{-}j)$	1–6	1–11	1–9	6–9	7–9	1–4	1–3
1	J_{ij} [16]	4.6	1.0	1.7	−0.45	−0.37	−1.55	−0.5
2	J_{ij} [18]	4.8	1.37	1.37	−0.5	−0.5	−1.6	−0.7
3	J_{ij} [19]	5.8	5.3	5.3	0.5	0.5	0.7	0.7
4	J_{ij} [58]	7.4	1.72	1.72	0	0	−1.98	0
5	J_{ij} [59]	10.25	10.17	10.17	1.98	1.98	−0.69	−0.69

Figure 2 shows the effective magnetic moment at a small external field of $B = 0.1$ T as a function of temperature. Data of Sessoli [27] and Murrie [60] are given by symbols. For

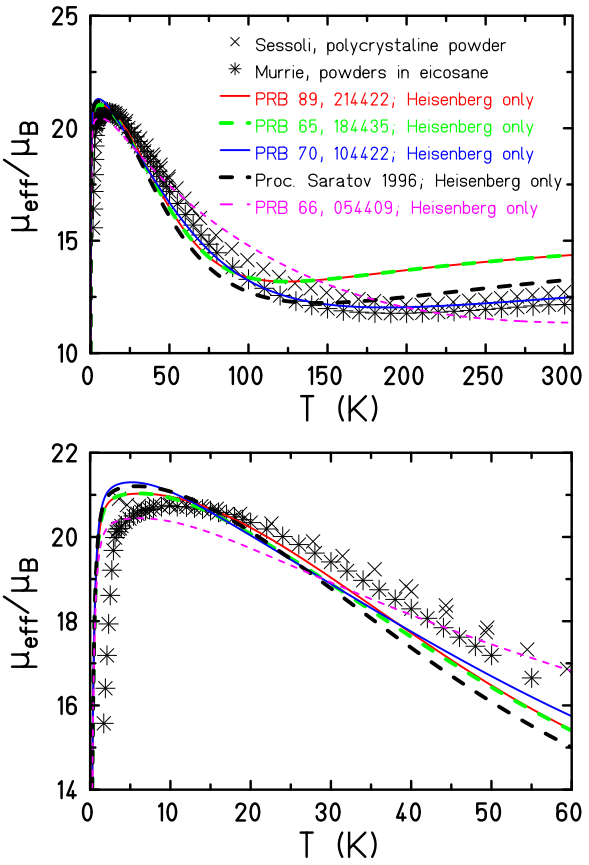

FIG. 2. (Color online) Effective magnetic moment of Mn_{12}-acetate at $B = 0.1$ T. Data of Sessoli [27] and Murrie [60] are given by symbols. Observables employing the Heisenberg part of parametrizations only are displayed by curves. The parametrizations correspond to those given in Table I from top to bottom.

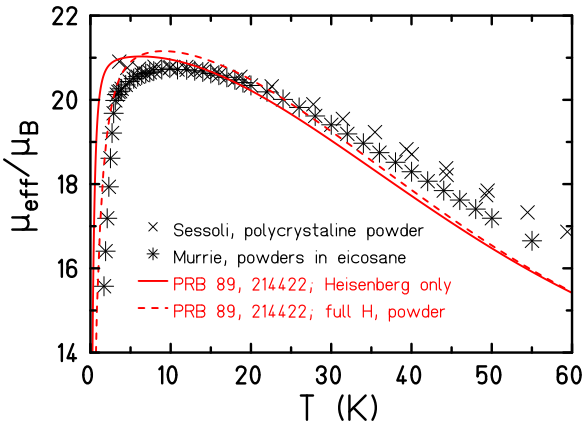

FIG. 3. (Color online) Effective magnetic moment of Mn_{12}-acetate at $B = 0.1$ T; same as Fig. 2. The dashed curve shows the result of a calculation employing the full Hamiltonian of Ref. [16]. The powder average is performed over a regular grid of 20 directions on the unit sphere [65].

the theory curves only the Heisenberg part of the respective parametrizations is used. Since the Heisenberg model is SU(2) symmetric, a FTLM version employing total $\underset{\sim}{S^z}$ symmetry was used with $R = 100$ and $N_L = 120$ in this case [40]. One realizes that the gross structure of the magnetic moment (which is proportional to $\sqrt{\chi T}$) is achieved by all parametrizations, especially at lower temperatures of $T \lessapprox 50$ K. A finer inspection shows that the maximum is at a too low temperature for all parametrizations, so that the experimental low-temperature data points are not met. For higher temperatures towards room temperature one notices that only one parametrization [19] (blue curve) closely follows the experimental data towards the paramagnetic limit. This is not astonishing since this parametrization was fitted to the high-temperature tail using a high-temperature series expansion. Since high-temperature series expansions allow rather accurate estimates of exchange parameters that are not altered by (small) anisotropic terms [61–64], one can consider the exchange parameters of Ref. [19] as good guidance. We thus conjecture that the somewhat too large effective magnetic moment of the DFT parametrizations [16,18] at room temperature are related to the fact that these parametrizations contain ferromagnetic interactions, whereas a fit to the high-temperature behavior [19] leads only to antiferromagnetic interactions (compare Table I). In addition, the antiferromagnetic interactions 1–11 and 1–9 are much stronger in Ref. [19].

Using the recently developed FTLM for anisotropic systems [42] we could calculate the effective magnetic moment starting from the DFT parametrization of Ref. [16]. Besides the Heisenberg terms of Table I, this parametrization contains anisotropic Dzyaloshinskii-Moriya interactions as well as full 3×3 anisotropy tensors for each manganese ion. It turns out that the additional terms improve the low-temperature data (compare Fig. 3). The maximum shifts towards the experimental position and the data points for smaller temperatures are much better approximated. But since the anisotropic terms are irrelevant for temperatures above 60 K, this does not cure the failure of the parametrization proposed in Ref. [16] for high temperatures, which is related to the exchange interactions that are more antiferromagnetic than estimated in Ref. [16].

IV. MAGNETIZATION AS A FUNCTION OF APPLIED FIELD

Low-temperature magnetization usually provides strong fingerprints of the underlying spin Hamiltonian, for instance, in the case of magnetization steps due to ground-state level crossings. For Mn_{12}-acetate the magnetization shows even richer characteristics, since below the blocking temperature a magnetic hysteresis is observed [23]. This exciting physical property turns out to constitute a problem when compared to theoretical equilibrium magnetization. Due to the long relaxation times, approximately 2800 h at $T = 2$ K [20], the experimental values do not necessarily reflect equilibrium values. On the other hand, the theoretical evaluation of nonequilibrium observables for a full spin model of Mn_{12}-acetate is totally out of reach.

Figure 4 provides two experimental data sets as well as various theoretical curves. The data set of Glaser [66] was taken on a powder sample, whereas the data set of Sessoli [27] was taken on a single crystal with a field in the direction of the tetragonal axis of the S_4 symmetric molecule. Both data sets coincide up to $B \approx 2.5$ T, and then the magnetization along the tetragonal axis jumps, whereas the powder signal smoothly increases with field. Already at this point it becomes clear that the measurements cannot reflect equilibrium properties, because the magnetization along the tetragonal axis, which is the easy axis of this strongly anisotropic molecule [67], cannot be the same as the powder-averaged magnetization.

Interestingly, all theory curves that rest on Heisenberg model calculations agree with each other perfectly, which is due to the fact that all produce a $S = 10$ ground state that is largely separated from excited levels. They also agree with the experimental magnetization up to a field of $B \approx 1$ T. Between 1 and 2.7 T the experimental data points stay below the theoretical curves. Above $B \approx 2.7$ T, theory and magnetization along the tetragonal axis meet again. The calculation for the full spin model of Mn_{12}-acetate as given in Ref. [16] yields a rather unexpected result: The powder-averaged magnetization

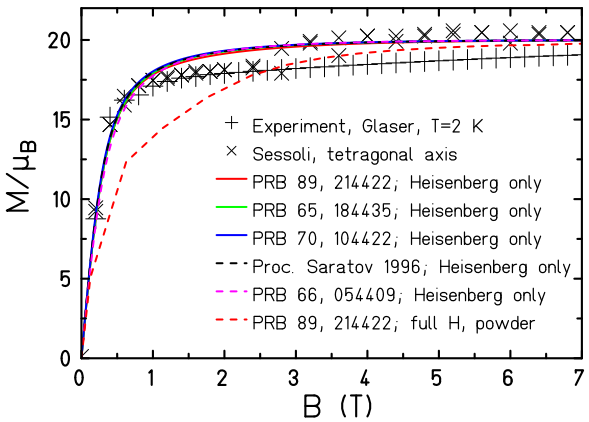

FIG. 4. (Color online) Magnetization of Mn_{12}-acetate at $T = 2$ K. Color code of curves as above. The dashed curve is evaluated for two field values per 1 T field interval only.

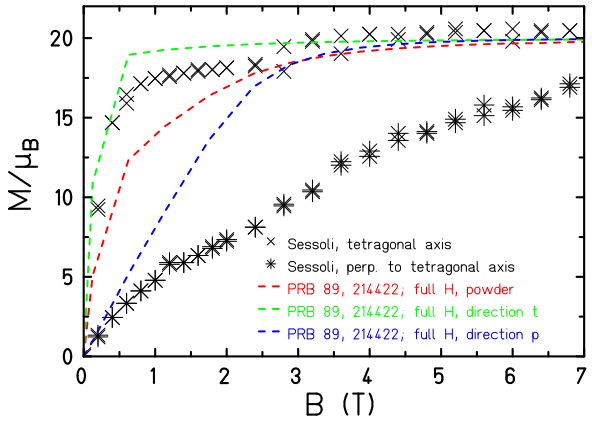

FIG. 5. (Color online) Magnetization of Mn_{12}-acetate at $T = 2$ K. The dashed curves are evaluated for two field values per 1 T field interval only. Direction $t = (0.0, -0.356\,82, 0.934\,17)$, direction $p = (-0.356\,82, 0.934\,17, 0.0)$.

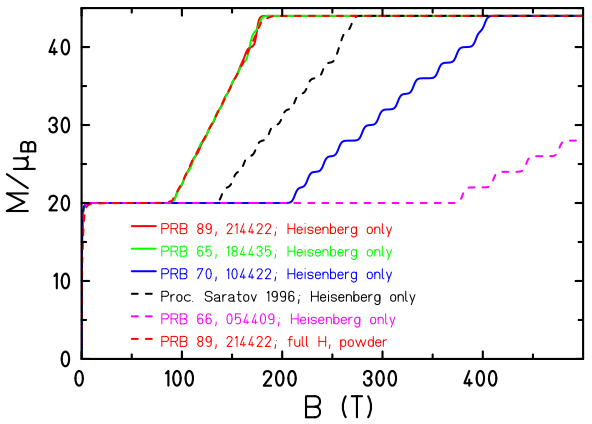

FIG. 6. (Color online) High-field magnetization of Mn_{12}-acetate at $T = 2$ K.

stays well below all other theory curves (expected since it is anisotropic), but also stays well below both experimental curves (unexpected at least compared to the experimental powder data).

In the following we compare our results with the measurements of Ref. [27] along two different directions, along the tetragonal axis and perpendicular to that, i.e., somewhere in the xy plane. Figure 5 presents three theory curves: one for the powder average and two along special directions. Direction $t = (0.0, -0.356\,82, 0.934\,17)$ points roughly along the tetragonal axis (inclination of about 20°) and direction $p = (-0.356\,82, 0.934\,17, 0.0)$ lies in the xy plane. Both theoretical curves show systematically larger magnetization values than the experiment. This could be for two reasons: Either the experimental curves are not in equilibrium, which is possible at $T = 2$ K where the relaxation time of Mn_{12}-acetate is long, or the parametrization of Ref. [16] is still not yet optimal, i.e., the **D** tensors could be too weak, for instance. In the DFT computation [16] the single-ion anisotropies of $Mn^{(III)}$ are of the order of 0.4 K, whereas in many other compounds values in the range of 1–4 K are observed [44–46,68–70].

Nevertheless, the positive message is that we can now calculate such curves and compare with experimental data. The theoretical costs, by the way, are still enormous—for the investigations shown in this paper, about 2 Mio. CPU hours on a supercomputer had to be used, since the FTLM procedure has to be completed twice for every field value and direction. Therefore, only a few field values have been used for the theoretical magnetization curves.

Finally, we would like to present the high-field magnetization curves. As can be seen in Fig. 6, the various parametrizations lead to distinctive differences at high fields. The high-field magnetization could be and has been measured in megagauss experiments [71]. Interestingly, the magnetization data given in Ref. [71] show pronounced features, likely related to magnetization steps, between 180 and 400 T, which could be compatible with the parametrization of Ref. [19] (blue curve in Fig. 6). As realized already by the authors, this parametrization produces a sequence of level crossings between the $S = 10$ ground manifold and the fully polarized state exactly in this field range.

V. HEAT CAPACITY

Another observable that was measured very early in the history of Mn_{12}-acetate is the heat capacity [25,72,73]. Figure 7 shows the experimental data of Ref. [25] for $B = 0$ (top) and $B = 0.3$ T (bottom). One notices that the heat

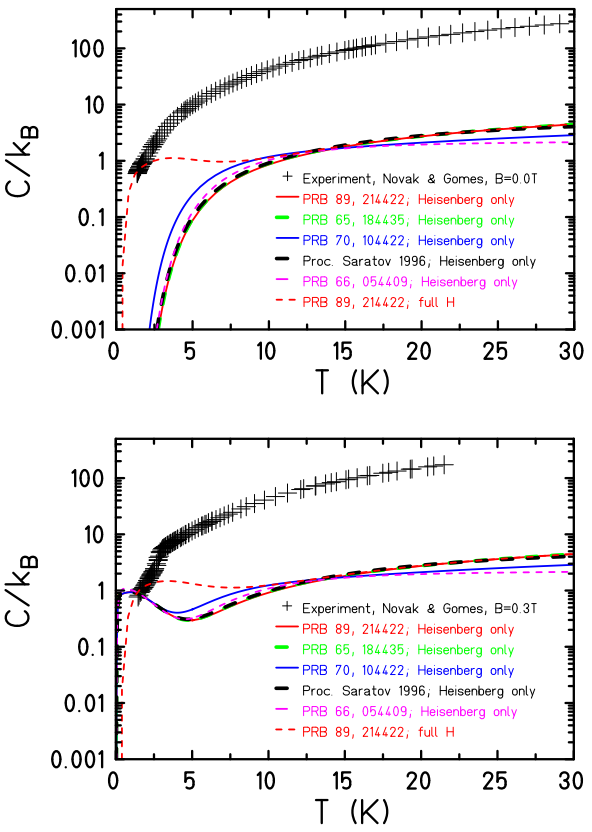

FIG. 7. (Color online) Specific heat of Mn_{12}-acetate at $B = 0$ (top) and $B = 0.3$ T (bottom). Data taken from Ref. [25]. Color code of curves as above. For $B = 0.3$ T the calculation for the anisotropic spin model was averaged over 20 directions.

capacity is rather large and grows steadily with temperature. This is due to a massive contribution from lattice vibrations (phonons) which grows as T^3. Therefore, the heat capacity data of magnetic molecules are usually overwhelmed by phonon contributions above $T = 5$ K.

This fact becomes obvious when comparing the theoretical heat capacity data in Fig. 7 for the Heisenberg parametrizations at $B = 0$. At low temperatures the theoretical values are two or more orders of magnitude smaller than the experimental ones, but for the calculation using the full anisotropic Hamiltonian [16], one notices that the low-temperature values agree very nicely. We think that this is due to a more smeared-out density of states at low energies in the anisotropic model, whereas for Heisenberg systems these levels belong to highly degenerate multiplets which lead to a different, i.e., much smaller, heat capacity.

Interestingly, a magnetic field of $B = 0.3$ T has a similar effect. It smears out the density of states due to Zeeman splitting. Therefore, even for the plain Heisenberg models, the low-temperature heat capacity increases, but still does not agree with the experimental data. For the anisotropic spin Hamiltonian [16] the low-temperature heat capacity does not change much and still agrees nicely with the experimental data. We conjecture that although the energy levels are moved around by the magnetic field, the overall structure of the density of states remains very similar. Summarizing, the specific heat is well reproduced by the anisotropic spin Hamiltonian of Ref. [16] for low temperatures around 1 K.

VI. SUMMARY AND OUTLOOK

Thirty-five years after its synthesis and 22 years after the first measurements [22] of Mn_{12}-acetate, the finite-temperature Lanczos method puts us in a position to evaluate thermodynamic functions of really large magnetic molecules. It thus complements DFT and other calculations of spin-Hamiltonian parameters for such big systems insofar in that one no longer needs to stop halfway to an understanding of thermodynamic observables.

In addition, one can now assess the quality of parametrizations for bigger spin systems. In the present case of Ref. [16], it turns out that although the range of addressed terms of the spin Hamiltonian is quite impressive, the agreement with magnetic observables is not yet optimal. We are of course aware of the fact that the mapping from an electronic Hamiltonian (in its DFT approximate treatment) to a spin Hamiltonian is a nontrivial task which is further complicated in cases where one encounters competing interactions, i.e., frustration. Such calculations are, for instance, much easier for even membered spin rings of $Fe^{(III)}$ ions, where neither frustration nor spin-orbit interactions play a role [74,75]. We are confident that the further development of DFT-based methods will be successful and that calculations such as the one presented here are helpful since they provide the necessary feedback.

In addition, this is a good example to teach us that one can get certain observables correctly modeled, such as the low-lying levels in Ref. [16] and the low-temperature magnetic moment, and still miss other observables, simply due to the large numbers of parameters which often are not independent of each other [76]. Since FTLM calculates equilibrium quantities only, the next major necessary step is now to develop tools for an evaluation of nonequilibrium properties of such big quantum spin systems.

ACKNOWLEDGMENTS

This work was supported by the Deutsche Forschungsgemeinschaft (DFG SCHN 615/15-1). Computing time at the Leibniz Computing Center in Garching is also gratefully acknowledged. We thank Roberta Sessoli, Mark Murrie, Thorsten Glaser, Stephan Walleck, Miguel Novak, and Angelo Gomes for providing their very valuable experimental data for comparison, and we thank Alexander Lichtenstein, Mikhail Katsnelson, Vladimir Mazurenko, as well as Roberta Sessoli for fruitful discussions.

[1] A. Liechtenstein, M. Katsnelson, V. Antropov, and V. Gubanov, Local spin density functional approach to the theory of exchange interactions in ferromagnetic metals and alloys, J. Magn. Magn. Mater. **67**, 65 (1987).

[2] E. Ruiz, P. Alemany, S. Alvarez, and J. Cano, Toward the prediction of magnetic coupling in molecular systems: Hydroxo- and alkoxo-bridged cu(ii) binuclear complexes, J. Am. Chem. Soc. **119**, 1297 (1997).

[3] J. Kortus, C. S. Hellberg, and M. R. Pederson, Hamiltonian of the V15 Spin System from First-Principles Density-functional Calculations, Phys. Rev. Lett. **86**, 3400 (2001).

[4] H. A. De Raedt, A. H. Hams, V. V. Dobrovitski, M. Al-Saqer, M. I. Katsnelson, and B. N. Harmon, Many-spin effects and tunneling splittings in Mn_{12} magnetic molecules, J. Magn. Magn. Mater. **246**, 392 (2002).

[5] D. W. Boukhvalov, E. Z. Kurmaev, A. Moewes, D. A. Zatsepin, V. M. Cherkashenko, S. N. Nemnonov, L. D. Finkelstein, Y. M. Yarmoshenko, M. Neumann, V. V. Dobrovitski, M. I. Katsnelson, A. I. Lichtenstein, B. N. Harmon, and P. Kögerler, Electronic structure of magnetic molecules V15: LSDA+U calculations, x-ray emissions, and photoelectron spectra, Phys. Rev. B **67**, 134408 (2003).

[6] T. Baruah, J. Kortus, M. R. Pederson, R. Wesolowski, J. T. Haraldsen, J. L. Musfeldt, J. M. North, D. Zipse, and N. S. Dalal, Understanding the electronic structure, optical, and vibrational properties of the Fe_8Br_8 single-molecule magnet, Phys. Rev. B **70**, 214410 (2004).

[7] O. Zaharko, J. Mesot, L. A. Salguero, R. Valentí, M. Zbiri, M. Johnson, Y. Filinchuk, B. Klemke, K. Kiefer, M. Mys'kiv, T. Strässle, and H. Mutka, Tetrahedra system $Cu_4OCl_6daca_4$: High-temperature manifold of molecular configurations governing low-temperature properties, Phys. Rev. B **77**, 224408 (2008).

[8] S. Zartilas, C. Papatriantafyllopoulou, T. C. Stamatatos, V. Nastopoulos, E. Cremades, E. Ruiz, G. Christou, C. Lampropoulos, and A. J. Tasiopoulos, A $Mn^{II}_6Mn^{III}_6$ single-strand molecular wheel with a reuleaux triangular topology: Synthesis, structure, magnetism, and dft studies, Inorg. Chem. **52**, 12070 (2013).

[9] K. Kuepper, C. Derks, C. Taubitz, M. Prinz, L. Joly, J.-P. Kappler, A. Postnikov, W. Yang, T. V. Kuznetsova, U. Wiedwald, P. Ziemann, and M. Neumann, Electronic structure and soft-x-ray-induced photoreduction studies of ironbased magnetic polyoxometalates of type $\{(M)M_5\}_{12}Fe^{III}{}_{30}$ (m = Mo^{VI}, W^{VI}), Dalton Trans. **42**, 7924 (2013).

[10] A. Chiesa, S. Carretta, P. Santini, G. Amoretti, and E. Pavarini, Many-Body Models for Molecular Nanomagnets, Phys. Rev. Lett. **110**, 157204 (2013).

[11] H. J. Silverstein, K. Fritsch, F. Flicker, A. M. Hallas, J. S. Gardner, Y. Qiu, G. Ehlers, A. T. Savici, Z. Yamani, K. A. Ross, B. D. Gaulin, M. J. P. Gingras, J. A. M. Paddison, K. Foyevtsova, R. Valenti, F. Hawthorne, C. R. Wiebe, and H. D. Zhou, Liquidlike correlations in single-crystalline $Y_2Mo_2O_7$: An unconventional spin glass, Phys. Rev. B **89**, 054433 (2014).

[12] K. S. Pedersen, G. Lorusso, J. J. Morales, T. Weyhermüller, S. Piligkos, S. K. Singh, D. Larsen, M. Schau-Magnussen, G. Rajaraman, M. Evangelisti, and J. Bendix, Fluoride-bridged $\{Gd^{III}{}_3M^{III}{}_2$ (M=Cr, Fe, Ga) molecular magnetic refrigerants, Angew. Chem., Int. Ed. **53**, 2394 (2014).

[13] S. Sanz, J. M. Frost, T. Rajeshkumar, S. J. Dalgarno, G. Rajaraman, W. Wernsdorfer, J. Schnack, P. J. Lusby, and E. K. Brechin, Combining complementary ligands into one framework for the construction of a ferromagnetically coupled $[Mn^{III}{}_{12}]$ wheel, Chem. Eur. J. **20**, 3010 (2014).

[14] S. K. Singh and G. Rajaraman, Probing the origin of magnetic anisotropy in a dinuclear $\{Mn^{III}Cu^{II}\}$ single-molecule magnet: The role of exchange anisotropy, Chem. Eur. J. **20**, 5214 (2014).

[15] Y. O. Kvashnin, O. Grånäs, I. Di Marco, M. I. Katsnelson, A. I. Lichtenstein, and O. Eriksson, Exchange parameters of strongly correlated materials: Extraction from spin-polarized density functional theory plus dynamical mean-field theory, Phys. Rev. B **91**, 125133 (2015).

[16] V. V. Mazurenko, Y. O. Kvashnin, F. Jin, H. A. De Raedt, A. I. Lichtenstein, and M. I. Katsnelson, First-principles modeling of magnetic excitations in Mn_{12}, Phys. Rev. B **89**, 214422 (2014).

[17] J. Kortus, T. Baruah, N. Bernstein, and M. R. Pederson, Magnetic ordering, electronic structure, and magnetic anisotropy energy in the high-spin Mn_{10} single molecule magnet, Phys. Rev. B **66**, 092403 (2002).

[18] D. W. Boukhvalov, A. I. Lichtenstein, V. V. Dobrovitski, M. I. Katsnelson, B. N. Harmon, V. V. Mazurenko, and V. I. Anisimov, Anisimov, Effect of local coulomb interactions on the electronic structure and exchange interactions in Mn_{12} magnetic molecules, Phys. Rev. B **65**, 184435 (2002).

[19] G. Chaboussant, A. Sieber, S. Ochsenbein, H.-U. Güdel, M. Murrie, A. Honecker, N. Fukushima, and B. Normand, Exchange interactions and high-energy spin states in Mn_{12}-acetate, Phys. Rev. B **70**, 104422 (2004).

[20] D. Gatteschi, R. Sessoli, and J. Villain, *Molecular Nanomagnets*, Mesoscopic Physics and Nanotechnology (Oxford University Press, Oxford, U.K., 2006).

[21] T. Lis, Preparation, structure, and magnetic properties of a dodecanuclear mixed-valence manganese carboxylate, Acta Crystallogr., Sect. B **36**, 2042 (1980).

[22] R. Sessoli, H. L. Tsai, A. R. Schake, S. Wang, J. B. Vincent, K. Folting, D. Gatteschi, G. Christou, and D. N. Hendrickson, High-spin molecules: $[Mn_{12}O_{12}(O_2Cr)_{16}(H_2O)_4]$, J. Am. Chem. Soc. **115**, 1804 (1993).

[23] R. Sessoli, D. Gatteschi, A. Caneschi, and M. A. Novak, Magnetic bistability in a metal-ion cluster, Nature (London) **365**, 141 (1993).

[24] L. Thomas, F. Lionti, R. Ballou, D. Gatteschi, R. Sessoli, and B. Barbara, Macroscopic quantum tunnelling of magnetization in a single crystal of nanomagnets, Nature (London) **383**, 145 (1996).

[25] A. Gomes, M. Novak, R. Sessoli, A. Caneschi, and D. Gatteschi, Specific heat and magnetic relaxation of the quantum nanomagnet Mn_{12}Ac, Phys. Rev. B **57**, 5021 (1998).

[26] A. Cornia, M. Affronte, A. C. D. T. Gatteschi, A. G. M. Jansen, A. Caneschi, and R. Sessoli, High-field torque magnetometry for investigating magnetic anisotropy in Mn_{12}-acetate nanomagnets, J. Magn. Magn. Mater. **226**, 2012 (2001).

[27] D. Gatteschi and R. Sessoli, Quantum tunneling of magnetization and related phenomena in molecular materials, Angew. Chem., Int. Ed. **42**, 268 (2003).

[28] R. Schnalle and J. Schnack, Numerically exact and approximate determination of energy eigenvalues for antiferromagnetic molecules using irreducible tensor operators and general point-group symmetries, Phys. Rev. B **79**, 104419 (2009).

[29] J. Jaklič and P. Prelovšek, Lanczos method for the calculation of finite-temperature quantities in correlated systems, Phys. Rev. B **49**, 5065 (1994).

[30] J. Jaklič and P. Prelovšek, Finite-temperature properties of doped antiferromagnets, Adv. Phys. **49**, 1 (2000).

[31] U. Manthe and F. Huarte-Larranaga, Partition functions for reaction rate calculations: Statistical sampling and MCTDH propagation, Chem. Phys. Lett. **349**, 321 (2001).

[32] M. W. Long, P. Prelovšek, S. El Shawish, J. Karadamoglou, and X. Zotos, Finite-temperature dynamical correlations using the microcanonical ensemble and the Lanczos algorithm, Phys. Rev. B **68**, 235106 (2003).

[33] M. Aichhorn, M. Daghofer, H. G. Evertz, and W. von der Linden, Low-temperature Lanczos method for strongly correlated systems, Phys. Rev. B **67**, 161103 (2003).

[34] A. Weiße, G. Wellein, A. Alvermann, and H. Fehske, The kernel polynomial method, Rev. Mod. Phys. **78**, 275 (2006).

[35] P. Prelovšek and J. Bonča, in *Strongly Correlated Systems*, edited by A. Avella and F. Mancini, Springer Series in Solid-State Sciences Vol. 175 (Springer, Berlin, 2013), Chap. 1.

[36] N. Shannon, B. Schmidt, K. Penc, and P. Thalmeier, Finite temperature properties and frustrated ferromagnetism in a square lattice Heisenberg model, Eur. Phys. J. B **38**, 599 (2004).

[37] I. Zerec, B. Schmidt, and P. Thalmeier, Kondo lattice model studied with the finite temperature Lanczos method, Phys. Rev. B **73**, 245108 (2006).

[38] B. Schmidt, P. Thalmeier, and N. Shannon, Magnetocaloric effect in the frustrated square lattice J_1-J_2 model, Phys. Rev. B **76**, 125113 (2007).

[39] M. Siahatgar, B. Schmidt, G. Zwicknagl, and P. Thalmeier, Moment screening in the correlated kondo lattice model, New J. Phys. **14**, 103005 (2012).

[40] J. Schnack and O. Wendland, Properties of highly frustrated magnetic molecules studied by the finite-temperature Lanczos method, Eur. Phys. J. B **78**, 535 (2010).

[41] J. Schnack and C. Heesing, Application of the finite-temperature Lanczos method for the evaluation of magnetocaloric properties of large magnetic molecules, Eur. Phys. J. B **86**, 46 (2013).

[42] O. Hanebaum and J. Schnack, Advanced finite-temperature Lanczos method for anisotropic spin systems, Eur. Phys. J. B **87**, 194 (2014).

[43] A. L. Barra, D. Gatteschi, and R. Sessoli, High-frequency EPR spectra of a molecular nanomagnet: Understanding quantum tunneling of the magnetization, Phys. Rev. B **56**, 8192 (1997).

[44] T. Glaser, M. Heidemeier, E. Krickemeyer, H. Bögge, A. Stammler, R. Fröhlich, E. Bill, and J. Schnack, Exchange interactions and zero-field splittings in C_3-symmetric $Mn^{III}_6Fe^{III}$: Using molecular recognition for the construction of a series of high spin complexes based on the triplesalen ligand, Inorg. Chem. **48**, 607 (2009).

[45] T. Glaser, M. Heidemeier, H. Theil, A. Stammler, H. Bögge, and J. Schnack, A Mn^{III} triplesalen-based 1D pearl necklace: Exchange interactions and zero-field splittings in a C_3-symmetric Mn^{III}_6 complex, Dalton Trans. **39**, 192 (2010).

[46] V. Hoeke, K. Gieb, P. Müller, L. Ungur, L. F. Chibotaru, M. Heidemeier, E. Krickemeyer, A. Stammler, H. Bögge, C. Schröder, J. Schnack, and T. Glaser, Hysteresis in the ground and excited spin state up to 10 T of a $[Mn^{III}{}_6Mn^{III}]^{3+}$ triplesalen single-molecule magnet, Chem. Sci. **3**, 2868 (2012).

[47] A. Bencini and D. Gatteschi, *Electron Paramagnetic Resonance of Exchange Coupled Systems* (Springer, Berlin, 1990).

[48] R. Boča, *Theoretical Foundations of Molecular Magnetism*, Current Methods in Inorganic Chemistry Vol. 1 (Elsevier, Amsterdam, 1999).

[49] N. L. Huang and R. Orbach, Biquadratic Superexchange, Phys. Rev. Lett. **12**, 275 (1964).

[50] U. Falk, A. Furrer, J. K. Kjems, and H. U. Güdel, Biquadratic Exchange in $CsMn_xMg_{1-x}Br_3$, Phys. Rev. Lett. **52**, 1336 (1984).

[51] R. Boca, Zero-field splitting in metal complexes, Coord. Chem. Rev. **248**, 757 (2004).

[52] J. Schnack, M. Brüger, M. Luban, P. Kögerler, E. Morosan, R. Fuchs, R. Modler, H. Nojiri, R. C. Rai, J. Cao, J. L. Musfeldt, and X. Wei, Observation of field-dependent magnetic parameters in the magnetic molecule Ni_4Mo_{12}, Phys. Rev. B **73**, 094401 (2006).

[53] A. Läuchli, G. Schmid, and S. Trebst, Spin nematics correlations in bilinear-biquadratic $s = 1$ spin chains, Phys. Rev. B **74**, 144426 (2006).

[54] R. Bastardis, N. Guihéry, and C. de Graaf, Microscopic origin of isotropic non-Heisenberg behavior in $s = 1$ magnetic systems, Phys. Rev. B **76**, 132412 (2007).

[55] R. Bastardis, N. Guihry, and C. de Graaf, Isotropic non-Heisenberg terms in the magnetic coupling of transition metal complexes, J. Chem. Phys. **129**, 104102 (2008).

[56] N. P. Konstantinidis, Zero-temperature configurations of short odd-numbered classical spin chains with bilinear and biquadratic exchange interactions, Eur. Phys. J. B **88**, 167 (2015).

[57] A. R. Farrell, J. A. Coome, M. R. Probert, A. E. Goeta, J. A. K. Howard, M.-H. Lemee-Cailleau, S. Parsons, and M. Murrie, Ultra-low temperature structure determination of a Mn_{12} single-molecule magnet and the interplay between lattice solvent and structural disorder, CrystEngComm **15**, 3423 (2013).

[58] B. Barbara, D. Gatteschi, A. A. Mukhin, V. V. Platonov, A. I. Popov, A. M. Tatsenko, and A. K. Zvezdin, in *Proceedings of Seventh International Conference on Megagauss Magnetic Field Generation and Related Topics*, edited by V. K. Cherynshev, V. D. Selemira, and L. N. Ilyashkevicha (VNIIEF Russian Federal Nuclear Center, Sarov, 1997), p. 853.

[59] N. Regnault, T. Jolicœur, R. Sessoli, D. Gatteschi, and M. Verdaguer, Exchange coupling in the magnetic molecular cluster $Mn_{12}Ac$, Phys. Rev. B **66**, 054409 (2002).

[60] P. Parois, The effect of pressure on clusters, chains and single-molecule magnets, Ph.D. thesis, University of Glasgow, 2010.

[61] H.-J. Schmidt, J. Schnack, and M. Luban, Heisenberg exchange parameters of molecular magnets from the high-temperature susceptibility expansion, Phys. Rev. B **64**, 224415 (2001).

[62] C. A. Thuesen, H. Weihe, J. Bendix, S. Piligkos, and O. Monsted, Computationally inexpensive interpretation of magnetic data for finite spin clusters, Dalton Trans. **39**, 4882 (2010).

[63] H.-J. Schmidt, A. Lohmann, and J. Richter, Eighth-order high-temperature expansion for general Heisenberg Hamiltonians, Phys. Rev. B **84**, 104443 (2011).

[64] A. Lohmann, H.-J. Schmidt, and J. Richter, Tenth-order high-temperature expansion for the susceptibility and the specific heat of spin-s Heisenberg models with arbitrary exchange patterns: Application to pyrochlore and kagome magnets, Phys. Rev. B **89**, 014415 (2014).

[65] J. Schnack, Magnetic response of magnetic molecules with non-collinear local d-tensors, Condens, Condens. Matter Phys. **12**, 323 (2009).

[66] T. Glaser and S. Walleck (private communication).

[67] M. A. Novak, R. Sessoli, A. Caneschi, and D. Gatteschi, Magnetic-properties of a Mn cluster organic-compound, J. Magn. Magn. Mater. **146**, 211 (1995).

[68] K. S. Pedersen, M. Schau-Magnussen, J. Bendix, H. Weihe, A. V. Palii, S. I. Klokishner, S. Ostrovsky, O. S. Reu, H. Mutka, and P. L. W. Tregenna-Piggott, Enhancing the blocking temperature in single-molecule magnets by incorporating 3d-5d exchange interactions, Chem. Eur. J. **16**, 13458 (2010).

[69] T. Glaser, Rational design of single-molecule magnets: A supramolecular approach, Chem. Commun. **47**, 116 (2011).

[70] J. Dreiser, K. S. Pedersen, A. Schnegg, K. Holldack, J. Nehrkorn, M. Sigrist, P. Tregenna-Piggott, H. Mutka, H. Weihe, V. S. Mironov, J. Bendix, and O. Waldmann, Three-axis anisotropic exchange coupling in the single-molecule magnets $NEt_4[Mn^{III}{}_2(5\text{-Brsalen})_2(MeOH)_2M^{III}(CN)_6]$ (M=Ru, Os), Chem. Eur. J. **19**, 3693 (2013).

[71] A. K. Zvezdin, I. A. Lubashevskii, R. Z. Levitin, V. V. Platonov, and O. M. Tatsenko, Phase transitions in megagauss magnetic fields, Phys.-Usp. **41**, 1037 (1998).

[72] J. F. Fernández, F. Luis, and J. Bartolomé, Time dependent specific heat of a magnetic quantum tunneling system, Phys. Rev. Lett. **80**, 5659 (1998).

[73] F. Luis, F. L. Mettes, J. Tejada, D. Gatteschi, and L. J. de Jongh, Observation of quantum coherence in mesoscopic molecular magnets, Phys. Rev. Lett. **85**, 4377 (2000).

[74] A. V. Postnikov, S. G. Chiuzbăian, M. Neumann, and S. Blügel, Electron spectroscopy and density-functional study of "ferric wheel" molecules, J. Phys. Chem. Solids **65**, 813 (2004).

[75] A. V. Postnikov, J. Kortus, and M. R. Pederson, Density functional studies of molecular magnets, Phys. Status Solidi B **243**, 2533 (2006).

[76] H.-J. Schmidt and M. Luban, Continuous families of isospectral Heisenberg spin systems and the limits of inference from measurements, J. Phys. A: Math. Gen. **34**, 2839 (2001).